Fracture mechanics parameters of narrow notches by experimental local displacement measurements

S. I. Eleonsky[1,a], Yu. G. Matvienko[2,b], I.N. Odintsev[2,b], V.S. Pisarev[1,a]

[1] Central Aero-Hydrodynamics Institute named after Prof. N.E. Zhukovsky (TsAGI).

1 Zhukovsky Street, Zhukovsky, Moscow Region 140180 Russia

[2] Mechanical Engineering Institute of the Russian Academy of Science

4 M. Kharitonievsky Per. 101990 Moscow, Russia

[a] dzuba@tsagi.ru, [b] ygmatvienko@gmail.com

Keywords: Stress intensity factor; T-stress; Crack compliance method; Local displacements; Electronic speckle-pattern interferometry; Narrow notch.

Abstract. New experimental technique for a determination of the stress intensity factor and the non-singular T-stress in the case of narrow notches is developed. The approach is based on combining the crack compliance method and optical interferometric measurements of local deformation response as a result of crack length increment. Initial experimental information has a form of in-plane displacement component values, which are measured by electronic speckle-pattern interferometry at some specific points located near the crack tip. The first four coefficients of Williams' formulation can be thus derived. A determination of initial experimental data in immediate neighbourhood of the notch tip is the main feature of the developed approach. In this case, it is not necessary to use complex numerical models which are connected with geometrical parameters and loading conditions of the object under study in a stage of experimental data interpretation. Moreover, an availability of high-quality interference fringe patterns, which are free from rigid-body motions, serves as a reliable indicator of real stress state in the vicinity of the notch tip. Proposed approach gives the unique capability for an estimation of the effect of the notch tip radius on fracture mechanics parameters. A confirmation of this fact is based on the investigation of U-notch increment for two notch radius (0.3 mm and 0.15 mm) in the same residual stress field. The values of the stress intensity factor and the T-stress are calculated for notches of different length. A difference in maximum values of K_I and T-stress is equal to 20% and 30%, respectively.

Introduction

Experimental determination of stress intensity factor (SIF) and T-stress for a crack of constant length under external load increment is of considerable current interest [1-8]. At the same time the crack compliance method is capable of SIF deriving by local crack length increasing under constant load conditions [9-10]. This presentation is devoted to a development and verification of new technique for a determination of SIF and T-stress values by combining the crack compliance method and optical interferometric measurements of local deformation response on a crack length increment. This approach is capable of estimating an influence of the notch radius on fracture mechanics parameters.

Main principals and relations

Modified version of the crack compliance method resides in recording interference fringe patterns, which correspond to a difference between two in-plane displacement component fields. Each field is referred to a crack of close but different length. The first exposure is made for a crack of initial length a_{n-1} (see Figure 1). Then initial crack length is increased by small

increment Δa_n so that new total crack length becomes equal to $a_n = a_{n-1} + \Delta a_n$ and the second exposure is performed. Required interference fringe patterns are visualized by numerical subtraction of two images recorded for two cracks [11]. Two interferograms, which are obtained by this way for thin plate with through edge crack of mode I, are shown in Figure 2. Positive direction of *x*-axis in Figure 1 and Figure 2 coincides with a direction of the crack propagation.

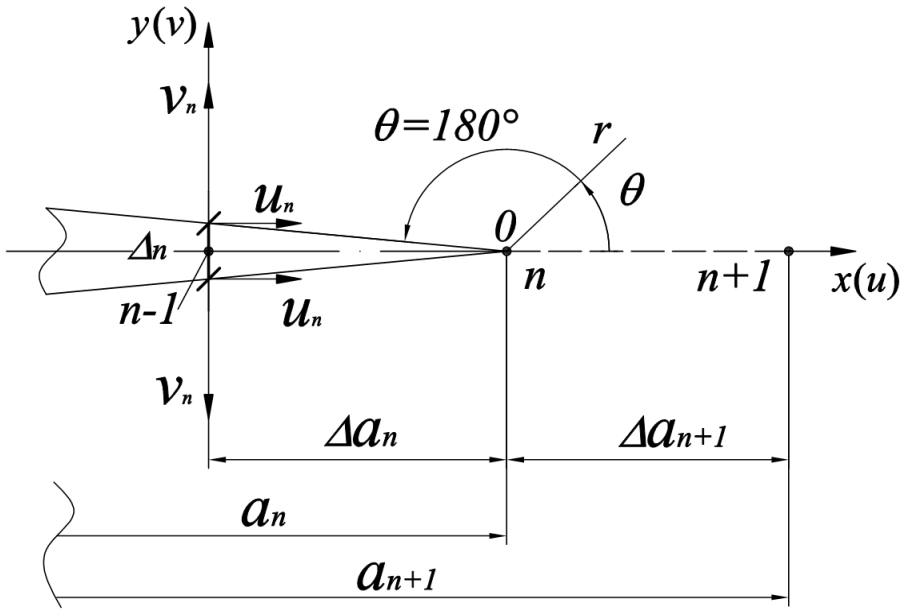

Fig. 1. Polar co-ordinate system related to the crack tip and the notation adopted.

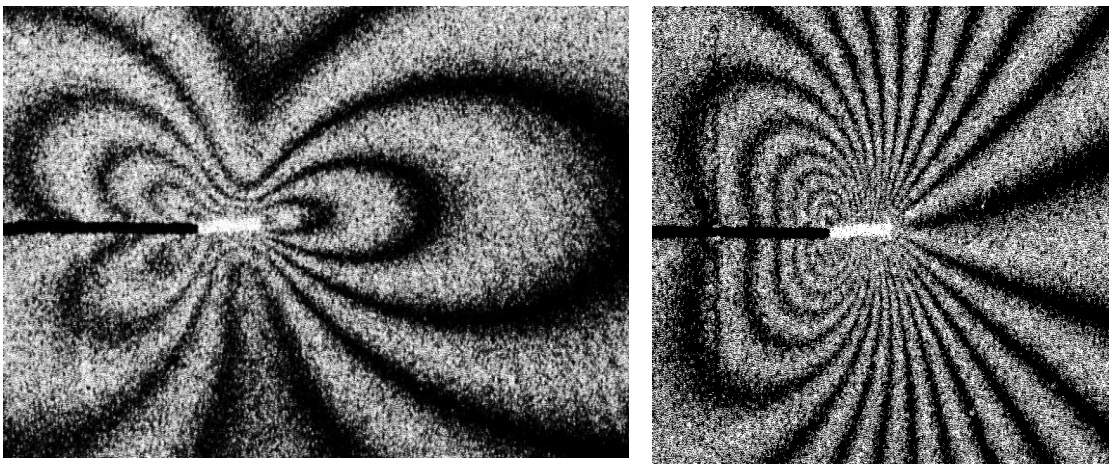

a b

Fig. 2. Specimen #2. Interference fringe pattern obtained
in terms of in-plane displacement component *u* (a) and *v* (b).
Initial crack length a_{14} = 28.5 mm with increment Δa_{15} = 1.7 mm;

Developed procedure for deriving required fracture mechanics parameters from interference fringe patterns is based on Williams' formulation [12]. Accordingly to this approach, displacement components at the crack tip proximity can be expressed as an infinite series for each in-plane displacement component. When *x*-direction coincides with the crack line the expressions for mode I crack have the following form:

$$u = \sum_{n=1}^{\infty} \frac{r^{\frac{n}{2}}(1+\mu)}{E} A_n \left\{ \left[k + \frac{n}{2} + (-1)^n \right] \cos\frac{n\theta}{2} - \frac{n}{2}\cos\frac{(n-4)\theta}{2} \right\},$$

$$v = \sum_{n=1}^{\infty} \frac{r^{\frac{n}{2}}(1+\mu)}{E} A_n \left\{ \left[k - \frac{n}{2} - (-1)^n \right] \sin\frac{n\theta}{2} + \sin\frac{(n-4)\theta}{2} \right\}, \quad (1)$$

where u and v are in-plane displacement component in direction of x and y axis, respectively; E is the elasticity modulus; μ is the Poisson's ratio; $k = (3 - \mu)/(1 + \mu)$ for plane stress and $k = (3 - 4\mu)$ for plane strain conditions; A_n are constants to be determined; r and θ are radial and angular distance from the crack tip as it shown in Figure 1.

Asymptotic formulation (1) gives the following form of elastic stress field for polar co-ordinate system with an origin at the crack tip [8]:

$$\sigma_{ij} = \frac{K_I}{\sqrt{2\pi r}} f_{ij}(\theta) + T\delta_{yi}\delta_{yj} + A_3\sqrt{2\pi r} + 0(r), \quad (2)$$

where K_I is the stress intensity factor; $f_{ij}(\theta)$ is the angular function based on formulae (1); δ_{ij} is the symbol of Kronecker's determinant. The second term is called the T-stress. The value of T is constant stress acting parallel to the crack plane in the direction of crack extension with a magnitude proportional to the applied gross stress. The third term A_3 is sometimes used as a transferability parameter like the T-stress. The non-singular term T represents a tension (or compression) stress. Positive T-stress strengthens the level of crack tip stress biaxiality and leads to high crack-tip constraint while negative T-stress leads to the lost of constraint. Values of K_I and T-stress are defined from relations (1) and (2) by the following way [7]:

$$K_I = A_1\sqrt{2\pi}, \quad T = 4A_2. \quad (3)$$

Generally initial experimental information represents a difference in absolute values of in-plane displacement components for two cracks of length a_n and a_{n-1}:

$$U_n = \hat{u}_n - \hat{u}_{n-1}, \quad V_n = \hat{v}_n - \hat{v}_{n-1}. \quad (4)$$

Relations (4) are valid for any point belonging to the proximity of crack tip located at point n. But right hand sides (4) include relative values of displacement components, which can not be used for direct determination of required A_n-values from decomposition (1). The key point of the developed approach resides in the fact that each interference fringe pattern of type shown in Figure 2 contains a set of specific points located at the crack border immediately. Absolute values of in-plane displacement components and then coefficients A_n from formulae (1) for a crack of a_n length can be determined at these points.

Specific points are located along the crack line between point n–1 and point n where displacement components $\hat{v}_{n-1}$ equal to zero before making a crack length increment. Thus interference fringe pattern shown in Figure 2b allows us a determination of absolute values of v-component for each point with polar co-ordinates $0 \le r \le \Delta a_n$ and $\theta = 180^o$. A distribution of v displacement component along the crack border ($\theta = 180^o$, see Figure 1), which corresponds to the first and the third terms of infinite series (1), is expressed as:

$$v(r,\theta=\pi)=\frac{4\sqrt{r}}{E}A_1-\frac{4r\sqrt{r}}{E}A_3+0(r). \tag{5}$$

Relation (5) shows that deriving K_I value from (3) demands a determination of v-values at two points belonging to the interval $0 \le r \le \Delta a_n$, $\theta = 180^o$, as minimum. The first of them is starting point of the crack increment. A substitution of $r = \Delta a_n$ and $v(\Delta a_n, \theta=180^o) = v_n$ in (5) gives:

$$2v_n=\Delta_n=\frac{8\sqrt{\Delta a_n}}{E}A_1^n-\frac{8\Delta a_n\sqrt{\Delta a_n}}{E}A_3^n, \tag{6}$$

where A^n_1 and A^n_3 are coefficients of decomposition (1) for a crack of a_n length. The second essential equation could be conveniently derived for the point with co-ordinate $r = \Delta a_n/2$. A substitution of $r = \Delta a_n/2$ and $v(\Delta a_n/2, \theta=180^o) = v^*_n$ in (5) gives:

$$2v_n^*=\Delta_n^*=\frac{8\sqrt{\Delta a_n}}{\sqrt{2}E}A_1^n-\frac{8\Delta a_n\sqrt{\Delta a_n}}{2\sqrt{2}E}A_3^n, \tag{7}$$

A value of stress intensity factor (SIF) K_I follows from solving the system of linear algebraic equations (6) and (7) and a substitution of obtained result into the first from relations (3):

$$K_I^n=\frac{E\sqrt{2\pi}}{8\sqrt{\Delta a_n}}\left\{2\sqrt{2}\Delta_n^*-\Delta_n\right\}. \tag{8}$$

Taking into account only the first term from (1) leads to well-known Westergaard relation:

$$K_I^n=\frac{\Delta_n E\sqrt{2\pi}}{8\sqrt{\Delta a_n}}. \tag{9}$$

A characterisation of T-stress values is based on a determination of u displacement component directed along the crack line. A distribution of u displacement component for points belonging to the crack border ($\theta = 180^o$, see Figure 1), which corresponds to the second and the fours terms of infinite series (1), is expressed as:

$$u(r,\theta=\pi)=-\frac{4r}{E}A_2+\frac{4r^2}{E}A_4+0(r). \tag{10}$$

Absolute value of u-component for a crack of a_n length can be again obtained at point n –1 with polar co-ordinates $r = \Delta a_n$ and $\theta = 180^o$. A substitution of $r = \Delta a_n$ and $u(\Delta a_n, \theta=180^o) = u_n$ in (10) leads to the following relation:

$$u_n=-\frac{4\Delta a_n}{E}A_2^n+\frac{4(\Delta a_n)^2}{E}A_4^n. \tag{11}$$

Relation (11) gives us the first equation essential for a determination of T-stress value. Note that all experimental parameters needed for equations (6), (7) and (11) can be derived from interferograms pair, which correspond to Δa_n crack length increment.

A formulation of the second required equation demands involving interference fringe pattern, which corresponds to crack length increasing from point n to point n+1 by Δa_{n+1} increment (see Figure 1). Absolute value of u-component at specific point n+1 with co-ordinates $r = \Delta a_{n+1}$ and $\theta = 0$ denoted as u_{n+1} depends on the first four coefficients of decomposition (1) by the following way:

$$u_{n+1} = \frac{2\sqrt{\Delta a_{n+1}}(1-\mu)}{E} A_1 + \frac{4\Delta a_{n+1}}{E} A_2^n + 2\Delta a_{n+1}\sqrt{\Delta a_{n+1}}\,\frac{(1-\mu)}{E} A_3^n + \frac{4(\Delta a_{n+1})^2}{E} A_4^n \,. \qquad (12)$$

Relation (12) represents the second equation essential for a determination of T-stress because values of coefficients A_1 and A_3 are already known from relations (6) and (7). Note that a value of u_{n+1} has to be derived from interference fringe pattern of type shown in Figure 2a, which are recorded for Δa_{n+1} crack length increment. If an estimation of T-stress value is restricted by coefficient A^n_2 only, the following simplified formula is valid:

$$T^n = -\frac{u_n}{\Delta a_n} E \,. \qquad (13)$$

T-stress value (13) can be determined by using interference fringe pattern of type shown in Figure 2a recorded for crack length increment Δa_n only.

Electronic speckle-pattern interferometry (ESPI) employs for a determination of in-plane displacement components [11]. Well-known optical system with normal illumination with respect to plane object surface and two symmetrical observation directions is used. When a projection of illumination directions onto plane surface of the investigated object coincides with ξ-direction, interference fringe pattern is described as:

$$d_\xi = N \frac{\lambda}{2\sin\Psi} \,, \qquad (14)$$

where d_ξ is in-plane displacement components in ξ-direction; $N = \pm1; \pm2; \pm3, \ldots$ are the absolute fringe orders; $\lambda = 0.532$ μm is the wavelength of laser illumination; $\Psi = 45^o$ is the angle between inclined illumination and normal observation directions. When ξ-direction coincides with x-axis and y-axis displacement component u and v can be derived accordingly to formula (14), respectively.

Experimental verification

Experimental verification of the developed approach is performed by using specially designed Specimen #2 made from 2024 aluminium alloy (E = 74000 MPa, μ = 0.33) shown in Figure 3. Working part of this specimen is a thin plate of dimensions 120x48x5 mm^3. A crack of length a_0 = 20 mm is initially made in the middle of the shortest side in a direction of the symmetry cross-section. The specimen is loaded by transverse force directed orthogonally to the crack line as it is shown in Figure 3. Step-by-step crack growth process is performed by narrow jewellery saw of 0.3 mm width that corresponds to notch radius ρ = 0.15 mm. Such a procedure is accompanied with recording interference fringe patterns, which correspond to a difference between initial and final states of the specimen with two cracks for close load value. A scheme of the experiment involved resides in the following. External transverse load P_{n1} is applied to the specimen. The first exposure is made for a crack of current length a_{n-1}. Then crack length is increased by small increment Δa_n and the second exposure is made for a crack of the final length $a_n = a_{n-1} + \Delta a_n$. During a process of crack length increasing a value of acting force is slightly decreased to P_{n2} due to a compliance of the force gage. Two interference fringe patterns recorded for 15th crack length increment are shown in Figure 2.

Interference fringe patterns are recorded for 21 crack length increments starting from initial crack length a_0 = 20 mm up to a_0+a_n = 60 mm. The most reliable results related to the same crack length increments and loading conditions are obtained for steps 15, 16 and 17. Initial experimental information obtained for these steps are listed in tables 1 and 2. The values of coefficients A^n_1, A^n_3 and stress intensity factors in table 1 correspond to relations (5)-(8). It should be specially note that SIF values obtained by formula (9) coincide with corresponding data from table 1 within 3 per cent because A^n_3 values are practically equal to zero. The latter

fact is valid for all steps considered. The values of coefficients A^n_2, A^n_4 and T-stresses obtained accordingly relations (11)-(12) are shown in table 2. An analysis of data presented in tables 1 and 2 leads to the following conclusions. First, SIF values are in five per cent agreement with the results of finite element simulation. Experimentally obtained SIF values are close to SIF values presented in work [7] for DCB specimen of dimensions 120x64x5 mm^3 made from 7010 T7651 aluminium alloy by digital image correlation (DIC) technique. In particular, for a crack of 40 mm total length and transverse load increment ΔP = 1 kN SIF-value is approximately equal to 7.4 MPa$\circ$m$^{0.5}$ and does not depend on number of terms of Williams' solution (1). The letter circumstance is also revealed in our investigation ($A^n_3 = 0$).

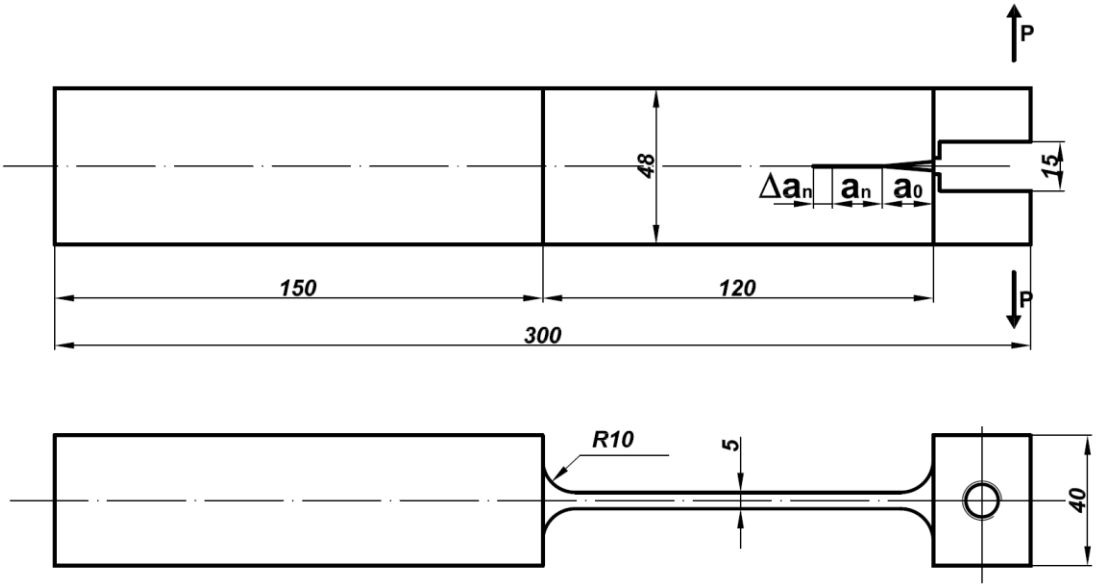

Fig. 3. Drawing Specimen #1MV and a scheme of its loading.

Table 1. Initial experimental information and SIF values for Specimen #2

Step n	P_{n1}, [kN]	P_{n2}, [kN]	Δa_n, [mm]	a_0+a_n, [mm]	Δ_n, [μm]	Δ^*_n, [μm]	A^n_1, [kg/mm$^{3/2}$]	A^n_3, [kg/mm$^{5/2}$]	K^n_I, [MPa$\circ$m$^{1/2}$]
15	0.64	0.60	1.7	50.2	11.9	8.4	8.4	0.0	6.7
16	0.64	0.60	1.7	51.9	12.5	8.7	8.6	–0.1	6.8
17	0.64	0.60	1.7	53.6	12.3	8.7	8.7	0.0	6.9

Table 2. Initial experimental information and T-stress values for Specimen #2

Step n	u_n, [μm]	u_{n+1}, [μm]	A^n_2, [kg/mm^2]	A^n_4, [kg/mm^3]	T^n, [MPa]	T^{n*}, [MPa]
15	–0.8	–2.3	–1.7	–1.5	–68	35
16	–0.8	–2.8	–1.5	–1.6	–76	35

An analysis of the accuracy of T-stress determination looks more difficult. First, used computer code is not capable of T-stress determination within appropriate accuracy. Second, the last column of table 2 includes T-stress values obtained by relation (13) denoted as T^{n*}. A difference in a sign and value of T-stresses obtained by solving a system of linear algebraic equations (11)-(12) and analogous data from relation (13) is evident. We believe that data, which correspond to terms A^n_2 and A^n_4, are more reliable. But T^{n*}-values have the same sign that analogous values from work [7]. Data obtained by DIC technique show that T-stress reaches maximal value T^2 =

16.5 MPa for the second term of formulae (1) and then slightly decreases with increasing the term number. Thus we have to conclude that revealed problems concerning a determination of the sign and value of T-stress proceeding from data of optical interferometric methods should be more carefully verified. To do this a wide set of additional experiments is currently performed. A set of experiments analogous to described above is performed for Specimen #1, which is completely analogous to Specimen #2, by using a cut of 0.52 mm width that approximately corresponds to notch radius ρ = 0.26 mm. Obtained SIF and T-stress values for both specimens coincide within 5 per cent interval.

Influence of the notch radius on fracture mechanics parameters

Developed approach is capable of determining fracture mechanics parameters for cracks in residual stress field. It is also possible to estimate an influence of the notch radius on SIF and T-stress values obtained through the use of relations (6)-(8) and (11)-(12), respectively. To do this a study of crack propagation in residual stress field near welded joint is performed. Two welded thin plates of dimensions 200x100x4 mm^3 made from aluminium alloy and denoted as Specimen #015 (cut width b_1 = 0.6 mm, notch radius ρ_1 ~ 0.30 mm) and Specimen #016 (cut width b_1 = 0.3 mm, notch radius ρ_2 ~ 0.15 mm) are investigated. Weld seam of lengths 100 mm coincides with one from symmetry cross-section of each specimen. Cracks in both specimens are propagated from a centre of the weld along the second symmetry cross-section in orthogonal to the weld direction. Preliminary determination of maximal residual stress values σ_y^{max} acting along the weld in both specimens serves for estimating an identity of residual stress fields. These values determined at points with co-ordinate x = 9 mm equal to σ_y^{max} = 130 and σ_y^{max} = 139 MPa for Specimen #015 and #016, respectively. Data are obtained by combining the hole drilling method and ESPI, with holes are drilled in specimen's area, which does not contain a crack.

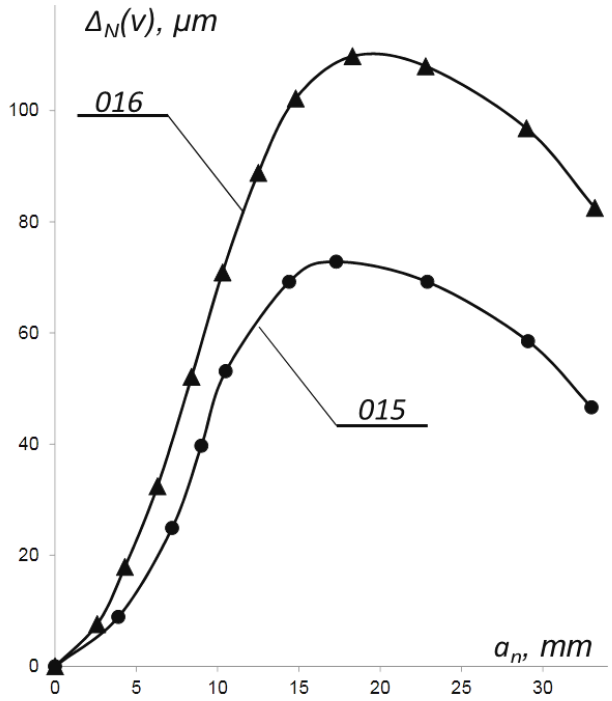

Fig. 4. Dependences of absolute crack opening form total crack length.

Experimental technique and a procedure of SIF and T-stress determination completely corresponds to the described above. Dependences of absolute crack opening form total crack length are shown in Figure 4. These curves are constructed by sequential summing each

individual crack opening Δ_n referred to starting point of crack length increment. A difference in maximal values of absolute crack opening for Specimen #015 ($\Delta_N(v)$ = 73 μm) and Specimen #016 ($\Delta_N(v)$ = 110 μm) equals to 34 per cent. Points, where each curve reaches its maximal value, practically coincide and correspond to crack length a_S = 16-18 mm. Dependences of SIF K_I and T-stress T values from total crack length are shown in Figure 5a and Figure 5b, respectively. These results show that co-ordinate of points where K_I = 0 and T = 0 do not depend on the notch radius and again correspond to crack length a_S = 16-18 mm. Maximal SIF values for Specimen #015 (K_I =14.3 MPa◦m$^{1/2}$) and Specimen #016 (K_I =17.8 MPa◦m$^{1/2}$) differ by 20 per cent. A difference in maximal values of T-stress for Specimen #015 (T = –120 MPa) and Specimen #016 (T = –188 MPa) reaches 30 per cent. T-stresses shown in Figure 5b are derived on a base of relations (11) and (12) It should be specially noted that formula (13) gives T = 0 for both specimens and any crack length increment.

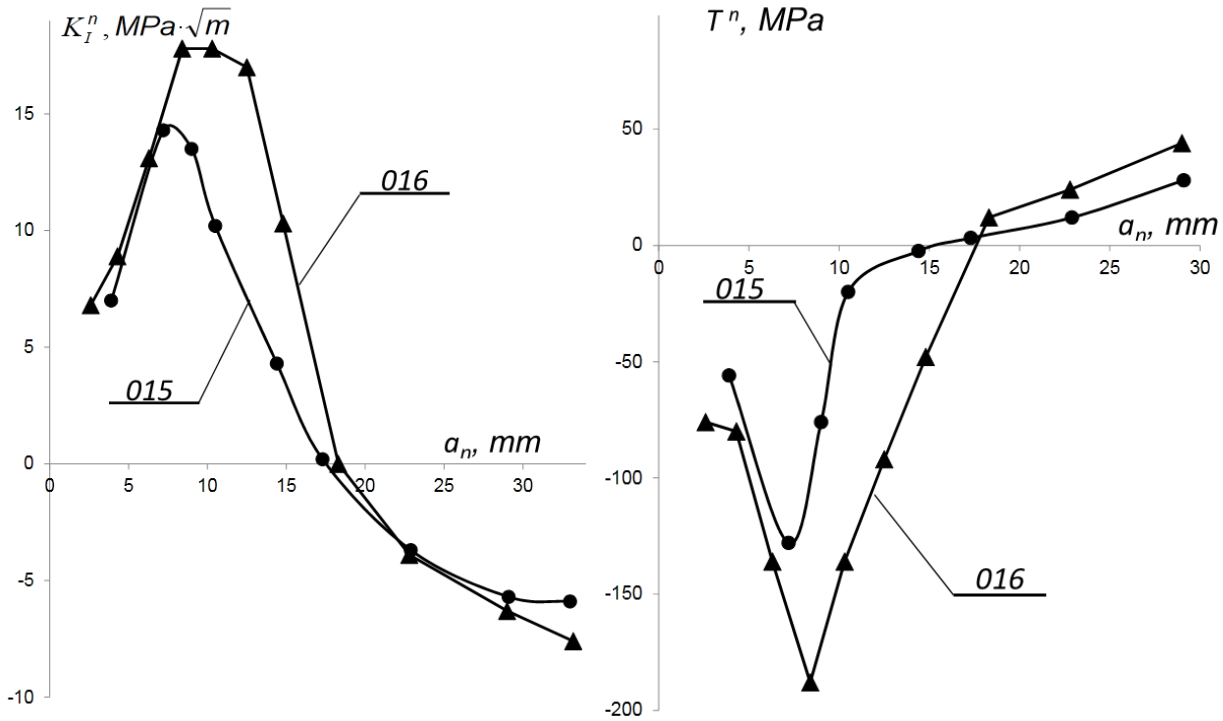

a b

Fig. 5. Dependences of SIF (a) and T-stress (b) values form total crack length.

Summary

New technique for a determination of fracture mechanics parameters is developed. Its essence resides in a measurement of local deformation response on small crack length increment by electronic speckle-pattern interferometry. Obtained experimental information is capable of deriving the first four coefficients of Williams' asymptotic series and further calculations of stress intensity factor and T-stress values. Developed approach allows us an estimation of dependencies of fracture mechanics parameters from a real width of the cut and/or U-notch radius. Two cases are considered for U-notches of radius ρ_1 ~ 0.30 mm and ρ_2 ~ 0.15 mm. The first of them is edge crack in specially designed specimen of DCB type. Performed study shows that there is no detectable difference in both SIF and T-stress values. The second case is the investigation of crack propagation in the same residual stress field for two notches of radius ρ_1 ~ 0.30 mm and ρ_2 ~ 0.15 mm. A difference in maximal values of K_I and T-stress is equal to 20 and 30 per cent, respectively.

Acknowledgement
Presented study is performed in the framework of RFFI Grant #10-08-00393-a and the Program of joint investigations of Central Aero-Hydrodynamics Institute and Mechanical Engineering Institute of the Russian Academy of Science.

References
[1] M.J. Maleski, M.S. Kirugulige, H.V and H.V. Tippur: Exp. Mech. Vol. 44 (2004), p. 522
[2] F. Hild, S. Roux: C. R. Mecanique, Vol. 334 (2006), p. 8
[3] S. Yoneyama, Y. Morimoto and M. Takashi: Strain Vol. 42 (2006), p. 21
[4] S. Yoneyama, T. Ogawa and Y. Kobayashi: Eng. Fracture Mech. Vol. 74 (2007), p. 1399
[5] J. Réthoré, S. Roux and F. Hild: Eng. Fracture Mech. Vol. 75 (2008), p. 3763
[6] P. López-Crespo, R.L. Burguete, E.A. Patterson, A. Shterenlikht, P.J. Withers and J.R. Yates: Exp. Mech. Vol. 49 (2009), p. 551
[7] J.R. Yates, M. Zanganeh and Y.H. Tai: Eng. Fracture Mech. Vol. 77 (2010), p. 2063
[8] M. Hadj Meliani, Z. Azari, G. Pluvinage G. and Yu. G. Matvienko: Eng. Fracture Mech. Vol. 77 (2010), p. 1682
[9] H.-J. Schindler: Int. Journal of Fracture Vol. 74 (1995), p. R23
[10] H.-J. Schindler, W. Cheng and I. Finnie: Exp. Mech. Vol. 37 (1997), p. 272
[11] P. Rastogi: *Digital speckle pattern interferometry and related techniques*, Wiley (2001)
[10] M.L. Williams: ASME Journal of Applied Mechanics Vol. 24 (1957), p. 109